


Effect of stochastic processes on structure formation in nanocrystalline materials under severe plastic deformation

Alexei Khomenko * and Daria Troshchenko

Department of Applied Mathematics and Complex Systems Modeling, Sumy State University, 40007 Sumy, Ukraine

Leonid Metlov

*Donetsk Institute for Physics and Engineering named after O.O. Galkin of the NASU, 03028 Kyiv, Ukraine
and Donetsk National University, 21021 Vinnytsia, Ukraine*



(Received 3 February 2019; published 7 August 2019)

Based on the nonequilibrium evolution thermodynamics, the structure refinement of metals during severe plastic deformation is investigated. To describe the formation of stationary (limiting) submicrocrystalline or nanocrystalline structures, a two-defect approximation, including the grain boundaries and dislocations, is used. Introduction of the additive noise for the main parameters into the governing equations allowed us to describe the self-consistent behavior of structural defects during the stationary structure formation. Conditions of achieving the stationary state are investigated and possible scenarios of structure refinement modes are determined. Obtained grain boundary density distributions help to estimate the composition of grain structure in the bulk of metal sample quantitatively. The analysis of time evolution of the grain boundaries density shows the presence of correlated fluctuations. The autocorrelation function, describing the frequency characteristics of the structure refinement, is determined.

DOI: [10.1103/PhysRevE.100.022110](https://doi.org/10.1103/PhysRevE.100.022110)

I. INTRODUCTION

The refinement of metallic structure along with other physical processes that occur in metals during severe plastic deformation (SPD) [1,2] can be described within recently developed approach of nonequilibrium evolution thermodynamics [3–5]. The approach combines the fundamental nonequilibrium thermodynamics principles and the Landau evolution equations [3–8]. It allows us to obtain the relations that correctly describe the evolution of defect subsystems and kinetics of the yield stress associated with it (strengthening). Also the theory can explain the grain refinement and the formation of stationary (limiting) submicrocrystalline (SMC) or nanocrystalline (NC) structure.

The independent thermodynamic variables in the set of evolution equations are the entropy and the densities of two defect types [dislocations and grain boundaries (GBs)]. The elastic strain tensor is a governing parameter. These variables are sufficient to describe unequivocally many fine details of grain structure refinement and accompanying processes. However, the fluctuations of the main parameters are not yet considered by the theory. These fluctuations can significantly change the nature of system evolution in some cases. For example, when the friction process of two atomically smooth mica surfaces separated by an ultrathin lubricant film and ice surface softening were investigated, the additive noise was pivotal in construing the stick-slip regime [9–12]. Note

that this mode has been observed experimentally, and its description is hard within the deterministic model [6–8].

The complete description of any physical process in real environment requires consideration of all possible internal interactions. However, the determination of the evolution of all separate elements of the macroscopic physical system is often an impossible task. Therefore, some approximations are necessary to model the physical phenomena or processes. In this case, the approximations take into account only the most significant influences and connections determining completely the nature of the process or phenomenon. At the same time, the deterministic models don't always correspond to reality. Neglected factors can contribute not only to a qualitative change in the behavior of the physical system, but even lead to the formation of new states. Since the effect of these unaccounted factors on the behavior of the system is random (stochastic), the system can make nonequilibrium transitions under the influence of stochasticity at any time. From the physical point of view this means that the system does not adapt its behavior to environment, but rather shows an active reaction.

As is well known, qualitatively new regimes and states can be formed as a result of self-organization processes [13,14]. Besides, only open and nonequilibrium systems, which interact with environment, can be self-organized. In that regard, the metallic structure formation at SPD occurs in strongly nonequilibrium conditions. This is because the grains refinement occurs so fast that the accompanying stresses do not have time to relax and the heat, generated as a result of work, does not have enough time to flow out of the system. Consequently, the system doesn't have the time-constant environment properties and evolves in random way. So, the process of the

*Also at Peter Grünberg Institut-1, Forschungszentrum-Jülich, D-52425 Jülich, Germany; o.khomenko@mss.sumdu.edu.ua; <http://personal.sumdu.edu.ua/khomenko/en/>

refinement of the polycrystalline sample and the formation of a stationary state has a stochastic nature. It is obvious that the fluctuations of the external field (external noise) are the main reason for the emergence of self-organization in a nonequilibrium system interacting with a thermostat. Since the intensity of the external noise doesn't depend on the size of the system, its influence predominates in comparison with the fluctuations of internal noise (fluctuations of the main state parameters). It leads later only to wander near the maxima of the effective internal energy [5]. It is known that in hierarchical systems, the additive noise of lower levels manifests itself as a multiplicative noise (it depends on the independent thermodynamic variables of the system) of higher level, which causes the appearance of additional phases and provides a transition between the stationary structures during SPD [9–14].

The main purpose of this work is to study the structural defects evolution during SPD considering the additive fluctuations of the basic parameters. Such a model should allow a more precise consideration of the refinement modes and the accompanied self-organization processes that cannot be achieved using deterministic approach [6–8]. Besides, the description of the transition from one stationary structure to another is carried out similarly to the Landau theory of equilibrium phase transitions [15] and the nonequilibrium models at constant values of the parameters of external influence [5]. Comparison of our model with other theories is carried out in introduction of work [6] (see also the literature cited therein).

The paper consists of four sections and conclusions.

The Sec. II presents the basic thermodynamic relations in terms of effective internal energy that allow to describe the formation of stationary (limiting) structures during SPD. The description of the resulting defect structures is carried out using the two-defect model taking into account the density of grain boundaries and dislocations, which define the formation of fine grained structure and a yield stress of plastic flow. For this purpose, the additional term in the power series expansion for the density of internal energy is introduced to represent self-consistent behavior.

The influence of the additive uncorrelated noise on the behavior of refinement processes is investigated in the Sec. III. Evolution equations of nonequilibrium variables of the system are obtained by direct differentiation of the multidimensional thermodynamic potential for the effective internal energy density. The equations uniquely reflect the specifics of the grain metal structure refinement and the accompanying processes during the SPD. Using the adiabatic approximation, that determines the nature of the evolution of the main nonequilibrium variables, the Langevin equation is obtained and the relation for the effective synergetic potential that allow observing the formation of various stationary (limiting) structures is constructed. A study of the stability loss of stationary states of the thermodynamic system is carried out. It allows to construct the phase diagram (PD) of metals or alloys refinement modes at SPD. The diagram establishes the conditions for the formation of stationary structures of different types and allows to generalize possible scenarios and modes of the behavior of the two-defect system. It allows to pinpoint specific parameters, which significantly affect the appearance of SMC or NC stationary (limiting) structure. It is shown

that distribution of the realization of GBs density allows to quantitatively estimate the composition of grain structure over the volume of metal sample. In the case of two stationary states or phases, the stationary structure of a metal can be determined by a mixture of grains of different sizes (at high level of fluctuations).

The kinetics of the evolution of GBs density is investigated in the Sec. IV. The time dependencies of GBs density are calculated, taking into account the fluctuations of the main parameters and demonstrating the dynamic rearrangement of the crystalline structure of metal or alloy during SPD. It has been found that, with sufficient intensity of fluctuations of a stochastic source, the system can experience dynamic transitions between states or phases of a material, corresponding to the stationary (limiting) structures with different grain sizes. Using the fast Fourier transform, a spectral analysis of the time dependencies is also performed. It is shown that the fluctuations spectrum in the metallic structure corresponds to the colored noise, which reflects the presence of correlated fluctuations in the system. Fluctuations are detected with the spectral power density of the signal, which is inversely proportional to the frequency and demonstrates the realization of $1/\omega^\alpha$, $0 < \alpha < 2$ or “pink” noise. It is found that the spectrum is related to the prehistory of nonequilibrium process of metals refinement during SPD. Autocorrelation function represents random fluctuations of GBs density and allows to reveal the frequency characteristics of refinement. It is exponential and demonstrates non-Markov behavior, since autocorrelation times are present in the system under certain conditions. The presence of weak correlation is shown. The results reflect the real refinement conditions and can be used for predicting the grain size or metal states (phases) during a certain autocorrelation time. Thus, it is possible to predict the necessary external conditions to achieve the desired stable SMC or NC structure.

Short conclusions of our investigation are given in the last Sec. V.

II. THERMODYNAMIC POTENTIAL IN TERMS OF NONEQUILIBRIUM EVOLUTION THERMODYNAMICS

As is well known, the mechanical work during SPD leads to the increasing of metal internal energy. The biggest part of work during cold processing goes towards the formation of structural defects and the heating of sample [5]. Two defect types, i.e., the GBs and dislocations, have the biggest influence on the processing flow. They establish the progress of refinement which is responsible for the formation of a yield stress of a metal [16,17]. Thus, the basic form of the effective internal energy density can be represented as a polynomial of the densities of the considered defect types:

$$u(h_g, h_D) = u_0 + \sum_{m=g,D} \left(\varphi_{0m} h_m - \frac{1}{2} \varphi_{1m} h_m^2 + \frac{1}{3} \varphi_{2m} h_m^3 - \frac{1}{4} \varphi_{3m} h_m^4 \right) + \varphi_{gD} h_g h_D - \psi_{gD} h_g^2 h_D, \quad (1)$$

where the value of index $m = g$ belongs to the GBs, while $m = D$ corresponds to the dislocations; h_g, h_D are the GBs and dislocations densities, it is believed that the average grain size

is approximately inversely proportional to the formed h_g (i.e., $d \sim 1/h_g$); u_0 , φ_{km} , φ_{gD} , ψ_{gD} are constant coefficients that reflect the reference level of the internal energy and the energy of defects interaction between each other and, respectively, with defects of other structural levels (i.e., they generally characterize system disequilibrium). The coefficients u_0 and φ_{km} ($k = 0, 1$), depending on the control parameter ε_{ij}^e (elastic strain), are defined as follows:

$$u_0 = \frac{1}{2}M(\varepsilon_{ii}^e)^2 + 2\mu I_2, \quad (2)$$

$$\varphi_{0m} = \varphi_{0m}^* + g_m \varepsilon_{ii}^e + \left[\frac{1}{2}\bar{M}_m(\varepsilon_{ii}^e)^2 + 2\bar{\mu}_m I_2 \right], \quad (3)$$

$$\varphi_{1m} = \varphi_{1m}^* + 2e_m \varepsilon_{ii}^e, \quad (4)$$

where $M = \lambda + 2\mu$ is a module of one-dimensional compression of material [18]; ε_{ii}^e , $I_2 \equiv (-\varepsilon_{ii}^e \varepsilon_{jj}^e + \varepsilon_{ij}^e \varepsilon_{ji}^e)/2$ are the first and second invariants of elastic strain tensor; positive constant g_m is responsible for the process of the structural defects generation at tension $\varepsilon_{ii}^e > 0$, or for their annihilation in case of compression $\varepsilon_{ii}^e < 0$; \bar{M}_m , $\bar{\mu}_m$ are elastic constants due to the existence of the defects in metal; e_m reflects the process of defects annihilation at positive value of $\varepsilon_{ii}^e > 0$ or generation in case of negative value of $\varepsilon_{ii}^e < 0$.

It should be noted, that the expression for the density of internal energy (1) takes into account the self-consistent behavior of the GBs h_g and dislocations h_D densities (the last term) in contrast to the assumed corresponding basic relationship in the papers [6–8]. This allows to describe the interaction of structural defects during the formation of stationary structures more accurately. The minus sign before this term is selected to guarantee the regularity of the expansion. It follows from the need to form stationary states (maxima of the thermodynamic or synergetic potential) due to the alternating signs of different powers of independent variables. From the physical point of view, this reflects the Le Chatelier principle, according to which a higher-level thermodynamic process is aimed at compensating for effects from thermodynamic processes of a lower level [19,20]. In addition, the introduced term further contributes to the appearance of the multiplicative resultant noise (a function of the independent thermodynamic variables), which causes the emergence of additional stationary states. The term specifies a transition between stationary structures [21–26].

Let us consider a simplified case. In the case of dislocations the power expansion (1) involves the dislocation density terms up to the second power only (herewith, $\varphi_{2D} = 0$ J m³, $\varphi_{3D} = 0$ J m⁵) [5,7]. The following set of coefficients was used in the numerical calculations:

$$\begin{aligned} \varphi_{0g}^* &= 0.4 \text{ J/m}^2, \quad g_g = 12 \text{ J/m}^2, \quad \bar{M}_g = 2.5 \times 10^5 \text{ J/m}^2, \\ \bar{\mu}_g &= 3 \times 10^5 \text{ J/m}^2, \quad \varphi_{1g}^* = 3 \times 10^{-6} \text{ J/m}, \quad e_g = 3.6 \times 10^{-4} \text{ J/m}, \\ \varphi_{2g} &= 5.6 \times 10^{-13} \text{ J}, \quad \varphi_{3g} = 3 \times 10^{-20} \text{ J m}, \quad \varphi_{0D}^* = 5 \times 10^{-9} \text{ J/m}, \\ g_D &= 2 \times 10^{-8} \text{ J/m}, \quad \bar{M}_D = 0 \text{ J/m}, \quad \bar{\mu}_D = 1.65 \times 10^{-4} \text{ J/m}, \\ \varphi_{1D}^* &= 10^{-24} \text{ J m}, \quad e_D = 6 \times 10^{-23} \text{ J m}, \quad \varphi_{gD} = 10^{-16} \text{ J}, \\ \psi_{gD} &= 10^{-23} \text{ J m}, \quad M = \mu = 2.08 \times 10^{10} \text{ Pa}. \end{aligned}$$

It corresponds to the phenomenological choice of constants corresponding to the observed regularities during the SPD

treatment [2,16,27,28]. The principles of this choice and the specific values of the coefficients are discussed in the paper [5]. This set of constants allows for a good compliance with the experimentally observed system behavior during SPD.

Note that, unlike dislocations, the contribution from the grain boundaries is taken into account up to the fourth power. This is because the GBs are topologically more complex defects, the third and fourth powers implicitly take into account the contribution of disclinations. Indeed, any grain is in contact with several grains and the simultaneous neighborhood of three grains is delimited by triple junction, which is essentially a disclination [29], i.e., a zone of excess energy from thermodynamic point of view. In the case of large grains (small h_g), the density of the triple junctions is low and their contribution to the total energy balance is small enough. In the case of small grains (large h_g), their contribution to the total energy balance is essential. In our procedure this contribution is taken into account not as an individual defect, but as an additional contribution from the third and fourth powers of the GBs density in the expansion of the effective internal energy Eq. (1). In fact, it is supposed that disclinations form a certain fine substructure of the GBs.

III. THE INFLUENCE OF ADDITIVE NOISE

Since white Gaussian noise is well suited for the mathematical description of physical processes, we investigate the influence of additive noise on the process of the formation of stationary structures. The set of evolution equations for the state parameters is [6–8,19]

$$\tau_{h_D} \frac{\partial h_D}{\partial t} = \varphi_{0D} - \varphi_{1D} h_D + \varphi_{gD} h_g - \psi_{gD} h_g^2 + N_D^{1/2} \xi_D(t), \quad (5)$$

$$\begin{aligned} \tau_{h_g} \frac{\partial h_g}{\partial t} &= \varphi_{0g} - \varphi_{1g} h_g + \varphi_{2g} h_g^2 - \varphi_{3g} h_g^3 + \varphi_{gD} h_D \\ &\quad - 2\psi_{gD} h_g h_D + N_g^{1/2} \xi_g(t), \end{aligned} \quad (6)$$

where τ_{h_m} are relaxation times (inversely proportional values to the kinetic coefficients). The stochastic addends are present in the right parts of the equations. They simulate the noise influence on the main parameters (internal noise) with the intensities N_D and N_g [13], which due to the influence of various structural inhomogeneities (substance phases, impurities, inclusions, interstitial defects, vacancies, structural defects of other levels, thermal fluctuations, etc.) and the influence of the external force. It is worth noting that close notations were developed in the mesoscopic nonequilibrium thermodynamics approach [30,31].

As is known, the SPD causes the formation of GBs of two types. The first one is a high-angle or geometrically necessary boundaries, which arise as a result of the various activity of the glide system around the GBs. The second type is cell boundaries or sub-boundaries, which are often called random dislocation boundaries. They correspond to random intersections of dislocations in the middle of the grains [18,32]. Accumulation of dislocations during the deformation gradually turns the cells into subgrains, which are limited by low-angle boundaries, and later become high-angle nanograins. Thus, the interaction of GBs with dislocations, other boundaries, and

structural inhomogeneities leads to the appearance of internal fluctuations and to change of the misorientation of the grain structure. With respect to the parameter h_g , it means that in the initial state a material has both coarse differently oriented grains and fine subgrains, which represent a static noise or chaos. The interaction of these grains at SPD processing establishes the competitive activity and the transitions between different structure states or phases. Considering h_D , the noise intensity N_D accounts for stochastic interaction of dislocation ensembles, which is accompanied by change of fluctuation spectrum and existence of collective effects (for example, the cellular structure formation [16,18,32,33]). The functions $\xi_i(t)$ ($i = D, g$) represent uncorrelated random Gaussian values. Their statistical moments are the following [34]:

$$\langle \xi_i(t) \rangle = 0, \quad \langle \xi_i(t) \xi_j(t') \rangle = 2\delta_{ij}\delta(t - t'), \quad (7)$$

where $\delta(x)$ stands for Dirac δ function and δ_{ij} is Kronecker δ symbol. The multiplier 2 in the second formula allows one to uniquely determine the form of the Fokker-Planck equation and give the expression $N(h_g)$ Eq. (10) meaning of the diffusion coefficient. In particular, the noise intensity (a measure of the fluctuations intensity) is included into the function $N(h_g)$.

Using the adiabatic approximation $\tau_{h_g} \gg \tau_{h_D}$, let us assume in Eq. (5) $\tau_{h_D} \dot{h}_D = 0$. After performing the transformations, we obtain a nonlinear equation of the Langevin-type:

$$\tau_{h_g} \dot{h}_g = F(h_g) + \sqrt{N(h_g)} \xi(t), \quad (8)$$

where $\xi(t)$ is resultant Langevin force (Gaussian white noise). The generalized force $F(h_g)$, which defines the kinetics of deterministic system, and the effective intensity $\sqrt{N(h_g)}$ of the fluctuations of a random variable [whose square determines the diffusion coefficient $N(h_g)$] are set by relationships:

$$F(h_g) \equiv \varphi_{0g} + \frac{\varphi_{0D}\varphi_{gD}}{\varphi_{1D}} + \left(\frac{\varphi_{gD}^2}{\varphi_{1D}} - 2\frac{\psi_{gD}\varphi_{0D}}{\varphi_{1D}} - \varphi_{1g} \right) h_g + \left(\varphi_{2g} - 3\frac{\psi_{gD}\varphi_{gD}}{\varphi_{1D}} \right) h_g^2 + \left(2\frac{\psi_{gD}^2}{\varphi_{1D}} - \varphi_{3g} \right) h_g^3, \quad (9)$$

$$N(h_g) \equiv \frac{(\varphi_{gD} - 2\psi_{gD}h_g)^2}{\varphi_{1D}^2} N_D + N_g. \quad (10)$$

The last one follows from the dispersion properties of Gaussian random variables [34]. It is obvious that $N(h_g)$ depends on the grain boundaries density h_g , therefore the noise in (8) has multiplicative character. It can lead to the nonequilibrium phase or structural transitions and to the formation of new system states (maxima of synergetic potential) that is hard within deterministic approach [6–8].

Since the solution of stochastic differential equation (SDE) with Langevin force (8), which has a normal distribution and δ -correlated autocorrelation function, cannot be obtained in closed form [34], only statistical characteristics of its solutions are usually considered. It is known that there are several forms of the Fokker-Planck equation, corresponding to the Langevin Eq. (8) [34–36]. In presented research, we use the Stratonovich interpretation [13]. This corresponds to the behavior of physical systems with continuous time and defines more real interpretation of the stochastic process $h_g(t)$

(the stochastic process with memory is considered). Note that numerical solution didn't demonstrate qualitative changes in the behavior of the system, when modeled using the Ito approach.

The corresponding Fokker-Planck equation is defined by the relationship

$$\frac{\partial}{\partial t} p(h_g, t) = -\frac{\partial}{\partial h_g} D^{(1)}(h_g) p(h_g, t) + \frac{\partial^2}{\partial h_g^2} D^{(2)}(h_g) p(h_g, t), \quad (11)$$

where the functions (the Kramers-Moyal coefficients) [34]

$$D^{(1)}(h_g) = \frac{F(h_g)}{\tau_{h_g}} + \sqrt{\frac{N(h_g)}{\tau_{h_g}^2}} \frac{d\sqrt{N(h_g)/\tau_{h_g}^2}}{dh_g}, \quad (12)$$

$$D^{(2)}(h_g) = \frac{N(h_g)}{\tau_{h_g}^2} \quad (13)$$

are drift and diffusion coefficients in Stratonovich interpretation, respectively. Equation (11) allows us to find the probability density $p(h_g(t))$ of the distribution of random values of h_g at any time t .

The distribution density of the solutions of Eq. (8) converges over time to a stationary form. This form can be found from Eq. (11) under the condition that $\partial p(h_g, t)/\partial t = 0$:

$$p(h_g) = Z^{-1} \exp[U_{ef}(h_g)], \quad (14)$$

which is determined by the normalization constant [37]

$$Z = \int_0^{+\infty} \exp[U_{ef}(\hat{h}_g)] d\hat{h}_g \quad (15)$$

and an effective synergetic potential

$$U_{ef}(h_g) = -\frac{1}{2} \ln[N(h_g)] + \tau_{h_g} \int_0^{h_g} \frac{F(\hat{h}_g)}{N(\hat{h}_g)} d\hat{h}_g, \quad (16)$$

which reflects the effective energy of the system and does not have the physical meaning of the internal energy.

It is obvious that distribution law (or the integral distribution law) of a continuous random variable h_g , i.e., the probability distribution function $F_p(h_g)$ is defined as

$$F_p(h_g) = \int_{-\infty}^{h_g} p(h_g) dh_g. \quad (17)$$

In Ref. [19] the stationary values for density of GBs h_g are determined with the help of the necessary condition for the extremum existence [$dp(h_g)/dh_g = 0$] of the distribution density Eq. (14) (or the effective synergetic potential Eq. (16), which is equivalent). At the same time, the maxima of the effective synergetic potential correspond to the maxima of the distribution density, which determine the formation of steady states (defect structures). Inversely, the minima correspond to unstable realizations.

Study of stability loss of the stationary states of the system, corresponding to the formation of the maxima of the effective synergetic potential $U_{ef}(h_g)$ Eq. (16) [or distribution density $p(h_g)$ Eq. (14)], allows to define the conditions of the formation of SMC or NC structures depending on both the change of the elastic strain I_2 (second invariant of the elastic strain tensor) and the intensity of noise the N_D (Fig. 1). Thus, the PD

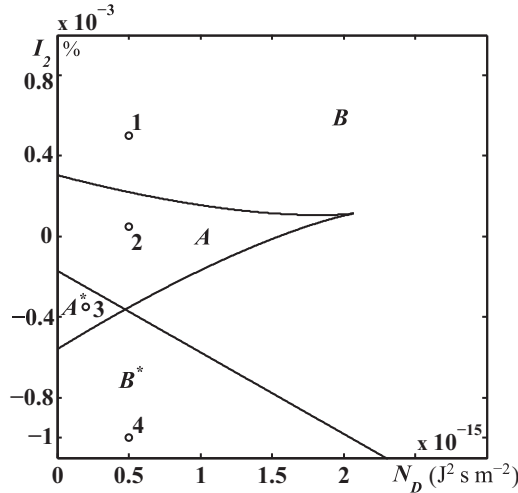


FIG. 1. Phase diagram of refinement regimes of polycrystalline metals or alloys at SPD at a constant value $\varepsilon_{ii}^e = -0.1\%$. Regions reflect the formation of two (A, A^*) and one (B, B^*) stationary (limiting) structures [19].

of metals or alloys refinement modes is obtained according to analytically found expressions for the distribution density $p[h_g(t)]$ and effective synergetic potential $U_{ef}(h_g)$ (Fig. 1).

According to the figure, the phase diagram has four regions of refinement regimes. Regions A, A^* demonstrate the possibility of the simultaneous formation of two stationary structures and regions B, B^* have only one stationary structure. In this case, the stationary structure with zero GBs density corresponds to elastic strains from the regions A^* and B^* . In other words, a zero maximum of $U_{ef}(h_g)$ (or the distribution density $p[h_g(t)]$) is formed. There is only one possible stationary state of the system in the case of B^* . For the case of A^* , the zero GBs density value has only the first stationary configuration.

The distribution density $p(h_g)$ Eq. (14) of random realizations of h_g during SPD and corresponding distribution law $F_p(h_g)$ Eq. (17) (integral distribution function of a random variable h_g), at the conditions indicated by the points 1–4 in the PD (Fig. 1), are shown in Fig. 2. Similarly to the determination of the effective synergetic potential, the distribution density of h_g in Fig. 2(a) is determined by the formation of a specified number of modes (maxima of probability distribution) [19,38]. These maxima (stable stationary states) arise depending on the behavior of applied load at SPD, which appears in the components of elastic strain tensor and is determined according to the PD regions. Thus, the curve 1 corresponds to the region B of large elastic strain in the PD (Fig. 1), where only one nonzero maximum $p(h_g)$ Eq. (14) can be realized. In this case, the maximum corresponds to the formation of NC stationary structure with the GBs density $h_g \approx 1.3 \times 10^7 \text{ m}^{-1}$ at probability $p(h_g) \approx 1.7 \times 10^{-7}$. The curve 2 characterizes the region A and corresponds to the formation of bimodal distribution density $p(h_g)$ Eq. (14). Besides, under certain conditions (values of I_2 and N_D) the system can simultaneously be in two metastable phases with large SMC (the first maximum at $p(h_g) \approx 5.7 \times 10^{-8}$ and $h_g \approx 1.4 \times 10^6 \text{ m}^{-1}$) and smaller NC grain sizes (the second maximum at $p(h_g) \approx 1.1 \times 10^{-7}$ and $h_g \approx 1.2 \times 10^7 \text{ m}^{-1}$) [22].

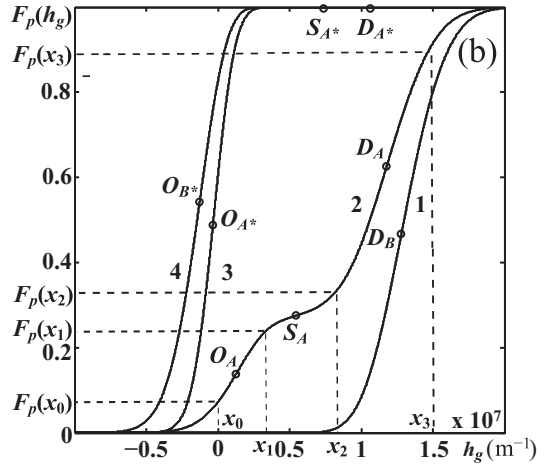
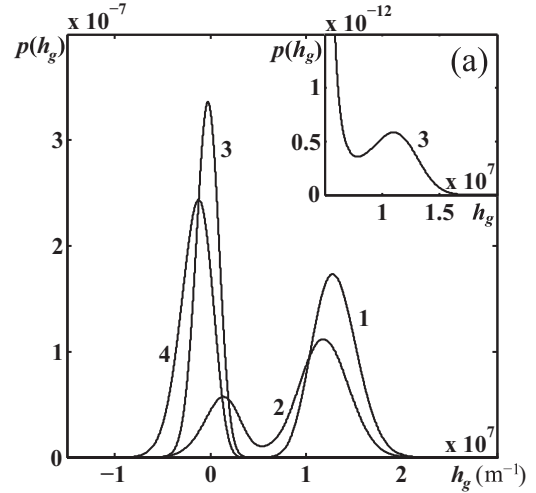


FIG. 2. The distribution of the GBs density in metallic structure at SPD. Panel (a) shows the function of distribution density $p(h_g)$ Eq. (14), while panel (b) represents the integral distribution law $F_p(h_g)$ Eq. (17). Curves 1–4 are built for corresponding points in the PD (Fig. 1) [38].

The probability of the formation of single stationary structure (the curve 4) in the region of small strains B^* takes the maximum value $p(h_g) \approx 2.4 \times 10^{-7}$ at $h_g = 0 \text{ m}^{-1}$. It corresponds to the formation of a coarse-grained polycrystal (monocrystal, in the limit). In the region A^* similarly to the region A in Fig. 1, the distribution density is bimodal with the probability $p(h_g) \approx 3.3 \times 10^{-7}$ and $p(h_g) \approx 5.8 \times 10^{-13}$ (the curve 3), but the first maximum is at zero value $h_g = 0$, while another reflects the formation of NC stationary structure with GBs density of $h_g \approx 1.15 \times 10^7 \text{ m}^{-1}$ (see inset). The curves 3 and 4 show the probability of the formation of stationary structures in the negative range of h_g , which has no physical meaning. It is considered that the density of GBs with negative h_g continues to function in a mode $h_g = 0 \text{ m}^{-1}$. It is obvious that, in a case presented by the curve 3, the system will spend most of its time in the first mode, because the probability of this is equal to $p(h_g) \approx 3.3 \times 10^{-7}$. This value is much higher than the probability of the formation of the second maximum. However, the possibility of such a structure formation in practice remains obscure.

Corresponding distribution law $F_p(h_g)$ Eq. (17) of the probability of a random value h_g is represented in Fig. 2(b). The points of curves 1–4 correspond to the formation of maximum (O_m , where $m = A, A^*, B^*$, and D_n , where $n = B, A, A^*$) and minimum (S_n , where $n = A, A^*$) values of distribution density $p(h_g)$ presented in Fig. 2(a). These extrema reflect the system states in suitable regions in the PD. The maxima are achieved at the points, where the distribution function has the biggest gradient or slope [look at the intervals (x_0, x_1) and (x_2, x_3) on the curve 2]. The minimum values of $p(h_g)$ of the curves 2, 3 in Fig. 2(a) are located near the center of shallow areas [see intervals (x_1, x_2) on the curve 2 in Fig. 2(b)]. The formation of steep areas of the curves 1–4 demonstrates the active refinement stages of metallic polycrystalline structure at SPD. Evolution speed of GBs density accepts the biggest value at these stages. In addition, the dependencies of $F_p(h_g)$ allow us to quantify the composition of grain structure of samples. It helps to evaluate the percentage of GBs density and approximate grain sizes in each interval of h_g values [39]. Thus, in a case presented by the curve 1, it is shown that GBs density is realized in the interval $[0.75 \times 10^7, 1.75 \times 10^7]$, which corresponds the approximate grain sizes $d \sim 57\text{--}133$ nm. The probability of the formation of stationary structure with the GBs density in this interval according to properties of distribution function is $p(0.75 \times 10^7 \leq h_g < 1.75 \times 10^7) = F_p(1.75 \times 10^7) - F_p(0.75 \times 10^7) \approx 0.95$ (95%). The probabilities that GBs density accepts the values within the intervals $[x_0, x_1]$ and $[x_2, x_3]$ (see the curve 2) are $p(x_0 \leq h_g < x_1) = F_p(x_1) - F_p(x_0) \approx 0.22 - 0.07 = 0.15$ (15%) and $p(x_2 \leq h_g < x_3) = F_p(x_3) - F_p(x_2) \approx 0.9 - 0.3 = 0.6$ (60%). The approximate grain sizes up to 285 nm and the range $d \sim 66\text{--}125$ nm correspond to these intervals. Obviously, the probability of the formation of an unstable configuration in the interval $[x_1, x_2]$ is $p(x_1 \leq h_g < x_2) = F_p(x_2) - F_p(x_1) \approx 0.3 - 0.22 = 0.08$ (8%). Since the system can simultaneously be (in different parts of the sample) in two phases, which are determined by a sharp slope of the curve 2, it is supposed that the sample as a whole will be defined by stationary (limiting) structure with a mixture of grains of different sizes [22]. That is, the bulk of SMC grains (to 285 nm) in the material structure is 15%, while nanosized grains (within $d \sim 66\text{--}125$ nm) are 60%, respectively. The cases presented by the curves 3 and 4 in Fig. 2(b) are given for complete analysis, because they show the formation of monocrystalline or coarse-grainy polycrystalline structures, which are not usually realized in metals at SPD.

Since the real refinement of metallic polycrystalline structure at SPD has a stochastic character and is subjected to the influence of state parameter fluctuations (the effect of internal noise), a stationary structure is formed with different proportion of bulk crystallites [22]. As a result, different mechanisms of plastic deformation are at work in the material. In the paper [18] an important role was assigned during SPD to the grain size distribution of ultra-fine-grained copper. It allowed to determine in-grain (subgrain) and grain-boundary processes in detail.

Thus, the PD, shown in Fig. 1, reflects the real conditions for the refinement of the polycrystalline structure at SPD, since it takes into account not only the influence of the external field, in the form of ε_{ii}^e and I_2 invariants of the elastic

strain tensor, but also internal mesoscopic fluctuations of N_D that can directly and critically affect the nature of the system evolution.

IV. TIME DEPENDENCIES OF GRAIN BOUNDARIES DENSITY

Let us investigate the kinetics of GBs density h_g , taking into account fluctuations of the main parameters $N_{D,g}$. The Langevin equation with multiplicative noise can be written in the stochastic differential form,

$$\tau_{h_g} dh_g = F(h_g)dt + \sqrt{N(h_g)} dW(t), \quad (18)$$

where $dW(t) = W(t + dt) - W(t) \equiv \xi(t)dt$ is the Wiener process, which has the properties of “white noise” [13,34,40]

$$\langle dW(t) \rangle = 0, \quad \langle (dW(t))^2 \rangle = 2dt. \quad (19)$$

Rewriting Eq. (18) more generally,

$$dh_g = D^{(1)}(h_g)dt + \sqrt{D^{(2)}(h_g)} dW(t). \quad (20)$$

Thus, the diffuse process is determined by the drift $D^{(1)}(h_g)$ and diffusion $D^{(2)}(h_g)$ coefficients that, within the Stratonovich (S-form) approach, satisfy the definitions Eqs. (12) and (13) [34].

Note that these coefficients provide the implementation of a single procedure for stochastic integration within the Ito calculus [13,34,41]. In this case, the representation of stochastic processes satisfies the Markov condition [that is, it demonstrates the independence of the increments $dW(t) = W(t + dt) - W(t)$]. Thus, the stochastic integral is defined as the Riemann-type integral that corresponds to the usual rules of mathematical analysis [13,34]. It is noteworthy that the presented forms of the calculus are interrelated and allow to make the mutual transformation [13,40,41]. If the original SDE (18) is given in the Stratonovich interpretation, then, taking into account the properties of Eq. (19), we can always go to the equivalent SDE in the Ito interpretation [42], subtracting the expression $g(h_g)dg(h_g)/dh_g$, where $g(h_g) = \sqrt{N(h_g)}/\tau_{h_g}^2$ [see drift coefficient determination Eq. (12)]. In turn, the reverse transition is performed by addition of $g(h_g)dg(h_g)/dh_g$. Thus, the original and equivalent forms of SDE have a single solution.

A numerical solution of Eq. (20) is found using the Euler method. Applying the discrete approximation of the differential of the random variable $dW(t) = \sqrt{\Delta t}W_i$, we obtain an iterative procedure for integrating Eq. (20),

$$h_{g_{i+1}} = h_{g_i} + D^{(1)}(h_{g_i})\Delta t + \sqrt{D^{(2)}(h_{g_i})\Delta t} W_i. \quad (21)$$

Using the definition of coefficients Eqs. (12), (13) and Eqs. (9), (10), we can compute the time evolution of the GBs density h_g .

The SDE (20) solution is found over the time interval $t \in [0, T]$ for a certain number of iterations N (the number of discrete points on the time dependence). Accordingly, the time step is $\Delta t = T/N$. The force W_i satisfies the following requirements:

$$\langle W_i \rangle = 0, \quad \langle W_i W_j \rangle = 0, \quad \langle W_i^2 \rangle = 2, \quad (22)$$

which correspond to the moments of white noise Eq. (19).

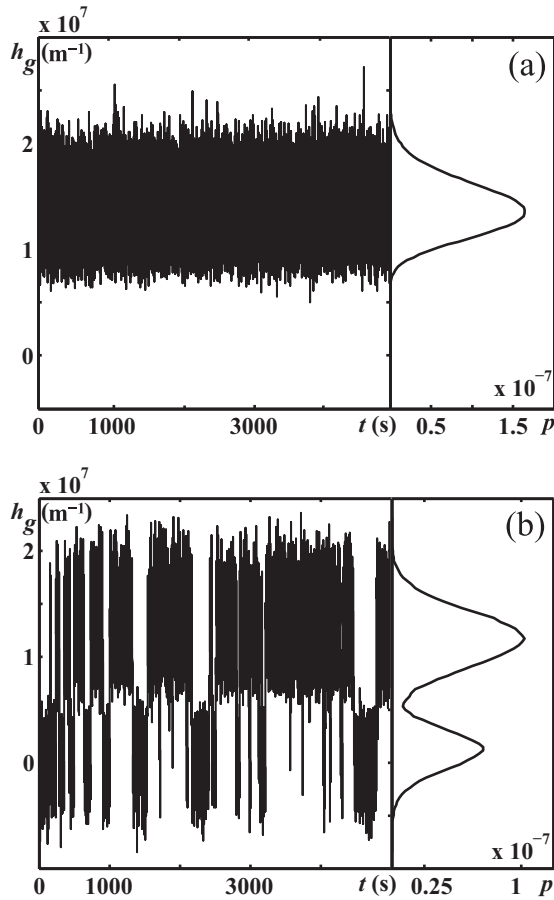


FIG. 3. Time dependencies $h_g(t)$ of the refinement modes in the regions (A, B) of the PD with the parameters $N_g = 1 \text{ J}^2 \text{ s m}^{-4}$, $\varepsilon_{ii} = -0.1 \%$, $N = 10^6$, $T = 5 \times 10^3 \text{ s}$, $\Delta t = 0.005 \text{ s}$. Panels (a) and (b) correspond to the points 1, 2 in the Fig. 1.

Evaluation of the random force, corresponding to the properties of white noise, is carried out using the Box-Muller model [43],

$$W_i = \mu \sqrt{-2 \ln r_1} \cos(2\pi r_2), \quad r_n \in (0, 1], \quad (23)$$

where, according to the second moment in Eq. (22), the variance is $\mu = \sqrt{2}$ and W_i is an absolutely random number that has properties Eq. (22). The pseudo-random numbers r_1 and r_2 have a uniform distribution and are repeated after a certain period.

Figure 3 shows the time series $h_g(t)$, obtained by numerical solution of Eq. (20). They determine the refinement modes of metallic structure during SPD according to regions (A, B) in the PD. The insets demonstrate the numerical probability distributions of the GBs density, which are found during the analysis of the obtained dependencies.

The presence of two stable stationary structures in the regions A and A* means that in a large sample under the same SPD treatment, both these stationary structures can be formed simultaneously in different areas of the sample with the probability, displayed in the inset to Fig. 3(b). Moreover, due to the fluctuation nature of the process, these areas can randomly transit from one stationary state to another and vice versa. It should be noted that the formation of two-mode

grain size distributions during SPD is actually observed in experiments [44–47]. In addition, one of the authors proposed a theory of the formation of a two-mode grain size distribution, based on a three-defect model (without taking in account fluctuation phenomena) [48]. In this model, small and large grains were formally considered as different types of defects. In addition, a simpler model, accounting for two defects and fluctuation phenomena, was considered in Ref. [49].

By definition, the maxima of the effective synergetic potential Eq. (16) and the probability density function $p(h_g)$ Eq. (14) correspond to the formation of stable stationary states (stationary structures). Thus, in the course of the numerical solution of the SDE (20), due to the action of a stochastic source, the system (that is, the grain boundaries density h_g) can generate large fluctuations around the stationary values and can transfer between these stable states with enough noise intensity. From Fig. 3 it can be seen that in the case of large elastic strains and fluctuations in the dislocation density with an intensity N_D determined in region B (see Fig. 1), the GBs density carries out intensive fluctuations around a single stationary state. This state corresponds to the average grain size $d \sim 76 \text{ nm}$. Accordingly, the NC structure is formed in the sample with grain sizes within the specified value. The elastic strain and intensity N_D from the region A (see Fig. 1) lead to the realization of random fluctuations around two stationary states. These states are determined by the size of the grains $d \sim 714 \text{ nm}$ and $d \sim 83 \text{ nm}$. Since the noise has a multiplicative nature, the noise-induced structural transformations occur constantly in the material during SPD. The stationary structure, which forms with time, has both SMC and NC grain sizes. Note that distributions of GBs density [see inset in Figs. 3(a) and 3(b)], which are built as a result of numerical analysis, completely coincide with the analytical dependencies $p(h_g)$ Eq. (14) in Fig. 2(a) (curves 1, 2).

From the physical point of view, fluctuations of the main parameters of the system state initiate the emergence of self-organizing processes that provide generation of new noise-induced states (phases) and contribute to change of the system properties during processing. It is known that structural transformations at SPD are characterized by some cyclicity. In particular, the stepwise structural transitions and corresponding changes in the properties of the sample are often observed in practice [3,16,21,23,24]. As was found in Ref. [50], during the refinement of metal sample, the process of plastic deformation has a recursive character, after the activation of dynamic recrystallization or amorphization. That is, the secondary refinement processes are generated in the arisen recrystallized grains or within the amorphous phase. Thus, the defects are accumulated under the stresses, which is accompanied by consequent transformations in the structure. In general, the structural transformations during SPD depend on factors such as: the temperature of processing, intensity and rate of deformation, concentration of impurities and structural defects of various levels, the dislocations ability to the diffusion rearrangement (the Peierls barrier), and the energy difference between the crystalline and amorphous states of the metal sample [3,51,52].

A spectral analysis of the time dependencies of the GBs densities $h_g(t)$ is performed and presented in Figs. 4(a) and 4(b). In particular, let us test them for the presence of

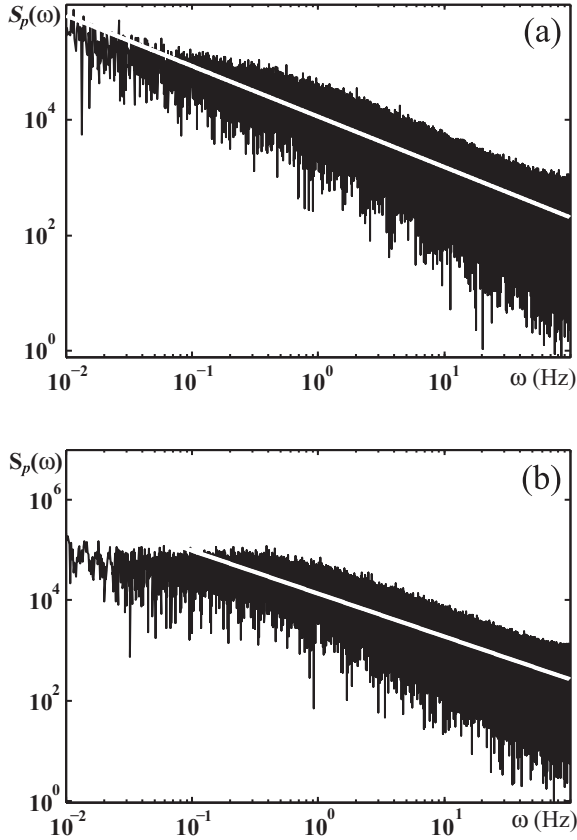


FIG. 4. The spectral density of the signal $S_p(\omega)$ for the refinement modes B (a) and A (b), which are shown in Fig. 3 at the sampling rate $\omega_n = 1/\Delta t$ Hz and the specified number 2^{20} of frequency bands (Fourier lines). White lines are defined by equations $S_p(\omega) \propto 1/\omega^{0.87}$ (a) and $S_p(\omega) \propto 1/\omega^{0.85}$ (b). Amplitude S_p is measured in conventional units.

harmonic components, which can arise due to the influence of a stochastic source (the effects of additive uncorrelated noise). The spectrum can be obtained using the Fourier transform [43]

$$S_p = \frac{1}{T} \int_0^T f(t) \exp(-i\omega t) dt, \quad (24)$$

where T is function $f(t)$ period, $\omega = 2\pi/T$ is frequency.

In this paragraph let us briefly introduce the discrete Fourier transform algorithm. To convert the problem into a discrete form the discrete instants of time $t_n = n\Delta t$ are introduced, where Δt is the sampling period. Further, the discrete values of the function at these instants of time $x_n = f(n\Delta t)$ are calculated or selected. In this case, the full period of the function is given by the product of the total number of points and the sampling period $T = N\Delta t$. Accordingly, the sampling rate of the signal takes on a value $\omega = 2\pi/T = 2\pi/(N\Delta t)$. Thus, performing mathematical transformations of expression (24), the definition of a discrete Fourier transform is obtained for a one-dimensional array x_n of length N ,

$$S_p = \frac{1}{N} \sum_{n=0}^{N-1} x_n \exp\left(\frac{-2\pi ink}{N}\right), \quad (25)$$

where $k = 0, \dots, N-1$ is the index of discrete Fourier transform in the frequency region [43].

So, let us analyze the time dependencies of the GBs density shown in Fig. 3. For calculation, we use the function `fft()` (Fast Fourier transform) in the MATLAB software environment. This function is based on the algorithm of the fast Fourier transform [43], which corresponds to the discrete transform, described above. It computes the spectrum of evolution $h_g(t)$, according to the relation Eq. (25). As a result, the function Eq. (25) returns a vector of complex numbers. Since the whole spectrum is equivalent to a positive part with a doubled amplitude, we reject negative frequencies (mirror image that does not contain information). Then performing normalization, we obtain the corresponding spectral dependencies of signal power $S_p(\omega)$ (Fig. 4).

The preliminary analysis of $S_p(\omega)$ in Fig. 4 shows that time dependencies $h_g(t)$ do not have the selected (significant) frequencies of their regular (periodic) components, since the maximum amplitudes in the signal spectrum are absent. The obtained dependencies are constructed at the sampling frequency $\omega_n = 1/\Delta t$ Hz and in accordance with a certain number 2^{20} of frequency bands (Fourier lines). Let us remind that corresponding time series in Fig. 3 are obtained by an iterative procedure Eq. (21) at $N = 10^6$, $T = 5 \times 10^3$ s, $\Delta t = 0.005$ s and reflect the refinement modes according to the regions (A, B) in the PD (Fig. 1).

It can be seen from Fig. 4 that the power of the signals spectrum $S_p(\omega)$ is almost identical irrespective of the refinement mode selection at SPD (the values of the control parameters in accordance with Fig. 1). Moreover, these dependencies decrease uniformly on a double logarithmic scale with an increase in the fluctuations frequency of the structural components in the metal sample. This means that fluctuations N_D have a high energy at low frequencies ω . In turn, the white lines, that approximate spectral dependencies using equations $S_p(\omega) = 1.14 \times 10^4 / \omega^{0.87}$ [see Fig. 4(a)] and $S_p(\omega) = 1.36 \times 10^4 / \omega^{0.85}$ [see Fig. 4(b)], also indicate a downward trend with increase of frequency. Only in the case shown in Fig. 4(b), we see that $S_p(\omega) \approx \text{const}$ at low frequencies (at $\omega < 0.5$ Hz), but the dependence decreases monotonically further. Thus, it is obvious that the spectrum (power) of fluctuations of the evolution variables will be determined by a single form (inversely proportional to the frequency) for all refinement modes of a metal sample under SPD. Therefore, different correlation times exist in the studied model.

It is known that most of the physical, biological and economic systems with phase transitions have stochastic (fluctuation) processes with power spectrum, which is inversely proportional to the frequency and is called $1/\omega$ noise, flicker noise or fractal-like (fractional) noise [40,53,54]. In particular, similar behavior occurs in many existing dynamical systems that have a source of “white” noise and are characterized by nonequilibrium transitions [53,55,56]. Besides, such pattern is observed during the so-called jerky plastic flow studied with the aid of the analysis of statistical distributions, fractal dimensions, and so on [57,58]. Moreover, the Fourier spectral analysis allowed to reveal $1/\omega$ noise even during macroscopically smooth plastic deformation [59].

Thus, spectrums roll-off is due to the fact that in the initial Langevin Eq. (8) nonlinear terms, that reflect interactions of nonequilibrium state parameters (structural defects of various

types), interfere with the realization of high frequencies. As a result, there is a transition from white noise $\xi(t)$, which characterizes most physical systems, to a colored one with a non-zero correlation time. In particular, the obtained values of the power exponent of fractional expressions ($\alpha = 0.85$ and $\alpha = 0.87$), which approximate the dependencies in Fig. 4, indicate that the system has a “pink” noise.

In general, “pink” noise has a power spectral density given by expression $S_p(\omega) \propto 1/\omega^\alpha$, where $0 < \alpha < 2$. This noise is very common in nature and takes an intermediate place between “white”, which has a spectrum of $S_p(\omega) \propto 1/\omega^0$, and “brown” or “red” noise with signal power that is inversely proportional to the square of the frequency ($S_p(\omega) \propto 1/\omega^2$) [40, 53–56]. In addition, it is known that “pink” noise reflects a process with memory like “brown” noise, that is, prehistory of the evolution of a random process is taken into account. While “white” noise has no memory.

Thus, the fluctuations spectrum in the metallic structure reflects the behavior of $1/\omega^\alpha$ or “pink” noise, which demonstrates the presence of correlated fluctuations in the system.

Let’s carry out an additional analysis of the random fluctuations of the GBs density h_g by constructing an autocorrelation function (ACF), which is determined for random processes by [60]

$$R(\tau) = E\{X(t)X^*(t - \tau)\}, \quad (26)$$

where $X(t)$ is the random process function (signal), E is the operator of mathematical expectation, the asterisk symbol denotes a complex conjugate value. It is known that ACF is used to analyze the complex oscillations. It is a useful characteristic of time dependencies, since it allows to study the existence of periodic components in the evolution and obtain their frequency characteristics. From the extreme values of obtained correlograms one can determine the corresponding correlation times in dynamical system. It is assumed that the autocorrelation dependence is periodic, if the initial function is periodic [60]. For a discrete time series with known mathematical expectation γ and variance μ , ACF is calculated as follows [60]

$$A_{cf}(\tau) = \frac{1}{N\mu^2} \sum_{t=1}^{N-\tau} (x_t - \gamma)(x_{t-\tau} - \gamma), \quad (27)$$

where N is a length of time series, τ is a lag or delay time.

Figure 5 shows autocorrelations of two functions depending on the time shift value τ . These dependencies are calculated from Eq. (27). Note that calculations of ACF are performed using the autocorr() function in the MATLAB software environment. The case, depicted in Fig. 5(a), shows a correlogram that is obtained as a result of numerical simulation of “white” noise. The dependencies displayed in Figs. 5(b) and 5(c) are constructed for the corresponding time dependencies of the evolution of GBs density in Fig. 3. It should be noted that to calculate ACFs in Figs. 5(b) and 5(c), time series obtained at $N = 10^6$, $T = 5 \times 10^4$ s, $\Delta t = 0.05$ s were used. This allowed us to evaluate more accurately the behavior of the dynamical system.

The figures show that ACFs decrease exponentially to zero (see inset) and exhibit insignificant damped oscillations

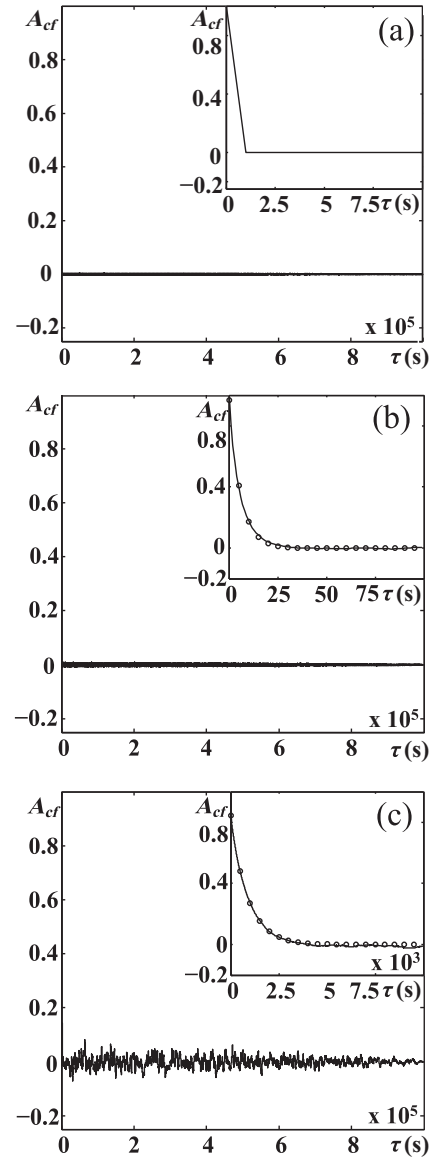


FIG. 5. Autocorrelation functions $A_{cf}(\tau)$ Eq. (27) of time dependencies. Panel (a) corresponds to the numerical representation of “white” noise. The correlations, as shown in panels (b) and (c), are constructed for the time dependencies of the GBs density under the conditions indicated in Fig. 3 and values $N = 10^6$, $T = 5 \times 10^4$ s, $\Delta t = 0.05$ s. Lines with circles are defined by equalities $A_{cf}(\tau) = 0.967 \exp(-0.172\tau)$ (b) and $A_{cf}(\tau) = 0.844 \exp(-0.001\tau)$ (c).

around the established value [12,61–63]. Thus, the periodicity in the obtained dependencies is not observed. Hence, the evolution of GBs density and autocorrelation in the system are formed randomly. But, as we can see, ACFs take on a stable value over time, which means the stationarity of time dependencies.

It can be seen from figures that ACFs assume the maximum value at $\tau = 0$ (that is, the correlation time is zero) in all cases. This meets the definition of an absolutely random process (that is, “white noise”), which has the Dirac function as ACF. However, comparing the results obtained in Figs. 5(b) and 5(c) (see inset) with the numerical approximation of δ -function in Fig. 5(a), it is apparent that investigated system has an

autocorrelation within a certain time interval. Thus, the set of Eqs. (8)–(10) is characterized by a non-Markov behavior. This pattern takes place due to the presence of colored noise with nonzero correlation time.

It is known that colored noise $\zeta(t)$ is described by the Ornstein-Uhlenbeck process [34], which is defined by

$$\tau \frac{d\zeta(t)}{dt} = -\zeta(t) + \xi(t), \quad (28)$$

where $\xi(t)$ is the representation of white noise with intensity $\sigma^2 = 1$ and moments

$$\langle \xi(t) \rangle = 0, \quad \langle \xi(t)\xi(t') \rangle = \sigma^2 \delta(t - t'). \quad (29)$$

In this case, the correlation function of the process $\zeta(t)$ has the form

$$\langle \zeta(t)\zeta(t') \rangle = \frac{\sigma^2}{2\tau} \exp\left(-\frac{|t - t'|}{\tau}\right), \quad (30)$$

where τ is autocorrelation time.

Approximation of the dependencies in Figs. 5(b) and 5(c) (see lines with circles in insets) gives equations like $A_{cf}(\tau) = 0.967 \exp(-0.172\tau)$ (case b) and $A_{cf}(\tau) = 0.844 \exp(-0.001\tau)$ (case c), that determine the form of ACFs. Thus, the evolution of the GBs density h_g depicted in Fig. 3 has an autocorrelation time $\tau \equiv 1/0.172 = 5.81$ s and $\tau \equiv 1/0.001 = 1000$ s. These values mean that the course of the evolution of the GBs density will more likely retain the tendency of a process during a certain period of time τ . It is known that correlation can have both a positive, if the trend of the process remains, and a negative effect, when reverse processes take place (for example, the alternation of increasing and decreasing dependence). Obviously, the relationship of the future with the history of the process is more pronounced, when the value of the autocorrelation time τ increases. Physically, we can forecast what size of grains in the sample will be at the next instant of time. That is, the appearance of predictable results of processing by SPD takes place.

In the case that meets the evolution of the GBs density in Fig. 5(c), it is supposed that autocorrelation time $\tau \equiv 1000$ s is an “effective,” since the system performs constant structural transformations. These transformations are expressed in the realization of dynamic transitions between two stationary structures (phases) with certain grain sizes. It is assumed that, under defined conditions and for a certain period τ , the system (metallic crystal structure) most likely (predominantly) functions in determined stationary state. According to the obtained distributions of GBs density (see Fig. 2) in the Sec. III, it means that stationary structure of a metal sample is determined by different proportion of bulk crystallites of certain size. Thus, it is possible to induce the formation of a preferred phase or stable structural state with an appropriate grain sizes in the stationary structure at subsequent times.

So, the analysis of ACFs has revealed that during the structure refinement of metals, a memory of the history of previous h_g or of generally stable states in the sample structure exists up to a certain point in time τ . Hence, it is possible to conclude that the magnitude of autocorrelation time affects the deviation of GBs density from the mean value. Consequently, the grain sizes, in the established stationary (limiting) structure, can assume different values under the same process-

ing conditions. In this regard, it is believed that the larger τ in the studied system (the crystal structure), the more time is required to process the metal sample to obtain the desired result. Thus, the results of our study can be useful from the technical point of view at setting the treatment conditions to achieve the desired outcome, that is, stable stationary structure with SMC or NC grain sizes.

V. CONCLUSIONS

Based on the nonequilibrium evolution thermodynamics, the refinement of metallic structure during severe plastic deformation is investigated. It is given information about the main modes of ordinary and intensive plasticity. The modeling of defect formation is carried out within two-defect model taking into account the noise. The grain boundaries and dislocations are considered as the main structural defects since they play an important role in the formation of fine-grained structures and yield stress of plastic flow.

Modification of the power series expansion for the density of effective internal energy allowed us to describe more accurately the self-consistent behavior of structural defects in the process of the formation of stationary (limiting) submicrocrystalline or nanocrystalline structures. The influence of additive uncorrelated noise of the main parameters is taken into account in the evolution equations. We assume that fluctuations of the main parameters reflect a stochastic interaction with other unaccounted structural inhomogeneities (phases of matter, impurities, inclusions, vacancies, structural defects of other levels, thermal fluctuations, etc.), which are always present in real metallic structures.

The investigation of the formation of system stationary states at elastic strain $\varepsilon_{ii}^e = -0.1$ % demonstrates the possible scenarios and modes of the refinement of polycrystalline structure. The distribution of grain boundaries density allows to estimate quantitatively the composition of grain structure over the volume of metal sample. Thus, one stationary structure with a probability of 95% and grain sizes within $d \sim 57$ – 133 nm can be formed under certain processing conditions. The stationary structure is determined by a mixture of grains of different sizes, subject to the simultaneous formation of two stationary states or phases. The bulk of submicrocrystalline grains with sizes up to 285 nm is 15%, while the nanocrystalline grains with sizes within $d \sim 66$ – 125 nm is 60% of the volume in metal sample. In addition, calculated time dependencies of the grain boundaries density demonstrate the process of rearrangement of the metallic crystal structure during severe plastic deformation. Thus, in the case of a single stationary state, the nanocrystalline structure with average grain size $d \sim 76$ nm is formed in a metal sample. Random transitions between two stationary states allow to form a fragmented structure with crystallites sizes $d \sim 714$ nm and $d \sim 83$ nm simultaneously. Moreover, the numerical calculation of the grain boundaries distribution corresponds well to the obtained here analytical dependencies. This result confirms the consistency between the Fokker-Planck equation and performed iteration procedure. Thus, the conducted study reproduces the real situation for severe plastic deformation and demonstrates the possible regimes and scenarios of metallic polycrystalline structure refinement.

The analysis of the time dependencies of grain boundaries density was carried out using a fast Fourier transform. Fluctuations are detected with the spectral power density, which is inversely proportional to the frequency and demonstrates the realization of $1/\omega^\alpha$ or “pink” noise. It showed the presence of correlated fluctuations in the system. It was found that the behavior of the spectrum is related to the prehistory of nonequilibrium process of metals structure refinement during severe plastic deformation. Research of autocorrelation function of h_g random fluctuations has allowed to reveal the frequency characteristics of refinement. Our results can be used for predicting the grain sizes or system states (phases) in metallic

structure during a certain correlation time τ . Moreover, it is possible to establish the necessary processing conditions to achieve the desired result (stable stationary structure with submicrocrystalline and/or nanocrystalline grain sizes).

ACKNOWLEDGMENT

The work was performed under the support of the Ministry of Education and Science of Ukraine within the framework of the project “Atomistic and statistical representation of formation and friction of nanodimensional systems” (Grant No. 0118U003584).

-
- [1] A. M. Glezer, *Bull. Russ. Acad. Sci. Phys.* **71**, 1722 (2007).
- [2] V. M. Segal, I. J. Beyerlein, C. N. Tome, V. N. Chuveldiev, and V. I. Kopylov, *Fundamentals and Engineering of Severe Plastic Deformation* (Nova Science Publishers, New York, 2010).
- [3] L. S. Metlov, *Phys. Rev. E* **81**, 051121 (2010).
- [4] L. S. Metlov, A. M. Glezer, and V. N. Varyukhin, *Russ. Metall.* **2015**, 269 (2015).
- [5] L. S. Metlov, *Phys. Rev. E* **90**, 022124 (2014).
- [6] A. V. Khomenko, D. S. Troshchenko, and L. S. Metlov, *Condens. Matter Phys.* **18**, 33004 (2015).
- [7] A. V. Khomenko and D. S. Troshchenko, in *Advances in Materials Science Research, Vol. 33*, edited by M. C. Wythers (Nova Science Publishers, New York, 2018), Chap. 9, pp. 231–273.
- [8] A. V. Khomenko, D. S. Troshchenko, and L. S. Metlov, *Metallofiz. Noveishie Tekhnol.* **39**, 265 (2017), (in Russian).
- [9] A. Khomenko, *Phys. Lett. A* **329**, 140 (2004).
- [10] A. V. Khomenko and I. A. Lyashenko, *Fluct. Noise Lett.* **7**, L111 (2007).
- [11] A. V. Khomenko and I. A. Lyashenko, *Phys.-Usp.* **55**, 1008 (2012).
- [12] A. Khomenko, *Tribol. Lett.* **66**, 82 (2018).
- [13] W. Horsthemke and R. Lefever, *Noise-Induced Transitions. Theory and Applications in Physics, Chemistry, and Biology* (Springer-Verlag, Berlin, 1984).
- [14] R. Thomson, M. Koslowski, and R. LeSar, *Phys. Rev. B* **73**, 024104 (2006).
- [15] L. D. Landau and E. M. Lifshitz, *Course of Theoretical Physics, Vol. 5: Statistical Physics* (Butterworth, London, 1999).
- [16] R. Z. Valiev, R. K. Islamgaliev, and I. V. Alexandrov, *Progr. Mater. Sci.* **45**, 103 (2000).
- [17] Y. Beygelzimer, V. Varyukhin, S. Synkov, and D. Orlov, *Mater. Sci. Eng. A: Struct.* **503**, 14 (2009).
- [18] E. V. Kozlov, N. A. Popova, and N. A. Koneva, *Russ. Metall.* **2015**, 264 (2015).
- [19] A. V. Khomenko, D. S. Troshchenko, Y. O. Kravchenko, and M. A. Khomenko, *J. Nano- Electron. Phys.* **9**, 03045 (2017) (in Ukrainian).
- [20] O. V. Yushchenko and A. Y. Badalyan, *Ukr. J. Phys.* **58**, 497 (2013).
- [21] Z. Zhang, M. Li, D. Guo, Y. Shi, X. Zhang, and H.-E. Schaefer, *Mater. Sci. Eng. A: Struct.* **594**, 321 (2014).
- [22] A. Zafari, X. S. Wei, W. Xu, and K. Xia, *IOP Conference Series: Mater. Sci. Eng.* **89**, 012055 (2015).
- [23] S. Jiang, Y. Zhang, L. Zhao, and Y. Zheng, *Intermetallics* **32**, 344 (2013).
- [24] W. Ma, B. Chen, F.-S. Liu, and Q. Xu, *Rare Metals* **32**, 448 (2013).
- [25] A. A. Goncharov, V. A. Kononov, G. K. Volkova, and V. A. Stupak, *Phys. Metals Metallogr.* **108**, 368 (2009).
- [26] A. D. Pogrebnyak, O. V. Bondar, S. O. Borba, G. Abadias, P. Konarski, S. V. Plotnikov, V. M. Beresnev, L. G. Kassenova, and P. Drodziel, *Nucl. Instrum. Meth. B* **385**, 74 (2016).
- [27] A. A. Mazilkin, B. B. Straumal, S. G. Protasova, O. A. Kogtenkova, and R. Z. Valiev, *Phys. Solid State* **49**, 868 (2007).
- [28] S. N. Sergeev, I. M. Safarov, A. V. Korznikov, R. M. Galeev, S. V. Gladkovsky, and E. M. Borodin, *Letters on Materials* **2**, 117 (2012) (in Russian).
- [29] A. E. Romanov and A. L. Kolesnikova, *Prog. Mater. Sci.* **54**, 740 (2009).
- [30] J. M. Rubi and A. Gadomski, *Physica A* **326**, 333 (2003).
- [31] A. Gadomski, J. Siodmiak, I. Santamaria-Holek, J. M. Rubi, and M. Ausloos, *Acta Phys. Pol. B* **36**, 1537 (2005).
- [32] G. Salishchev, S. Mironov, S. Zherebtsov, and A. Belyakov, *Mater. Phys. Mech.* **26**, 42 (2016).
- [33] V. V. Malashenko, *Phys. Solid State* **56**, 1579 (2014).
- [34] H. Risken, *The Fokker-Planck Equation. Methods of Solution and Applications* (Springer-Verlag, Berlin, 1989).
- [35] H. Haken, *Information and Self-Organization. A Macroscopic Approach to Complex Systems*, 2nd ed. (Springer-Verlag, Berlin, 2000).
- [36] Y. L. Klimontovich, *Phys. Usp.* **37**, 737 (1994).
- [37] The limits of integration are limited to the physical interpretation of the parameter h_g .
- [38] A. V. Khomenko, D. S. Troshchenko, I. O. Solonar, and P. E. Trofymenko, Modeling the noise influence on the metals fragmentation modes at severe plastic deformation, in *Proceedings of the IEEE 7th International Conference on Nanomaterials: Application and Properties (NAP'17)* (IEEE, USA, 2017), Vol. 6, p. 01PCSI12-1-5.
- [39] The obtained values show how many percents of the GBs density will be formed in a varying range.
- [40] C. W. Gardiner, *Stochastic Methods*, 4th ed. (Springer-Verlag, Berlin, 2009).
- [41] W. T. Coffey and Y. P. Kalmykov, Langevin Equations and Methods of Solution, in *The Langevin Equation* (World Scientific, Singapore, 2017), Chap. 2, p. 189, 4th ed.
- [42] Subsequently, for unambiguous perception, the form of the SDE calculus is interpreted in accordance with the initial interpretation (that is, in the form of Stratonovich) and regardless of the representation of stochastic processes.

- [43] W. H. Press, S. A. Teukolsky, W. T. Vetterling, and B. P. Flannery, *Numerical Recipes: The Art of Scientific Computing* (Cambridge University Press, New York, 2007).
- [44] Q.-W. Jiang and X.-W. Li, *Mater. Sci. Eng. A: Struct.* **546**, 59 (2012).
- [45] F. A. S. J. Poggiali, R. B. Figueiredo, M. T. P. Aguilar, and P. R. Cetlin, *Mater. Res.* **15**, 312 (2012).
- [46] O. Sedivy, V. Benes, P. Ponizil, P. Kral, and V. Sklenicka, *Image Anal. Stereol.* **32**, 65 (2013).
- [47] I. G. Brodova, I. G. Shirinkina, A. N. Petrova, O. V. Antonova, and V. P. Pilyugin, *Phys. Metals Metallogr.* **111**, 630 (2011).
- [48] L. S. Metlov, I. G. Brodova, V. M. Tkachenko, A. N. Petrova, and I. G. Shirinkina, *Phys. Metals Metallogr.* **118**, 1255 (2017).
- [49] L. S. Metlov, *Fiz. Tekhn. Vysokikh Davleniy* **29**, 28 (2019) (in Russian).
- [50] S. A. Firstov, N. I. Danilenko, V. I. Kopylov, and Y. N. Podrezov, *Russ. Phys. J.* **45**, 251 (2002).
- [51] B. B. Straumal, O. A. Kogtenkova, F. Muktepavela, K. I. Kolesnikova, M. F. Bulatov, P. B. Straumal, and B. Baretzky, *Mater. Lett.* **159**, 432 (2015).
- [52] N. V. Prodanov and A. V. Khomenko, *Surf. Sci.* **604**, 730 (2010).
- [53] S. Kogan, *Electronic Noise and Fluctuations in Solids* (Cambridge University Press, Cambridge, 1996).
- [54] I. V. Ovchinnikov, R. N. Schwartz, and K. L. Wang, *Mod. Phys. Lett. B* **30**, 1650086 (2016).
- [55] K. Syamal, K. Prodyot, and K. Jürgen, *Complex Dynamics in Physiological Systems: From Heart to Brain*, 1st ed., Understanding Complex Systems (Springer Netherlands, Berlin, 2009).
- [56] V. N. Skokov, V. P. Koverda, and A. V. Reshetnikov, *J. Exp. Theor. Phys.* **92**, 535 (2001).
- [57] M. A. Lebyodkin, I. V. Shashkov, T. A. Lebedkina, K. Mathis, P. Dobron, and F. Chmelik, *Phys. Rev. E* **88**, 042402 (2013).
- [58] M. A. Lebyodkin, I. V. Shashkov, T. A. Lebedkina, and V. S. Gornakov, *Phys. Rev. E* **95**, 032910 (2017).
- [59] R. N. Mudrock, M. A. Lebyodkin, P. Kurath, A. J. Beaudoin, and T. A. Lebedkina, *Scripta Mater.* **65**, 1093 (2011).
- [60] G. Box, G. Jenkins, G. Reinsel, and G. Ljung, *Time Series Analysis: Forecasting and Control*, 5th ed., Wiley Series in Probability and Statistics (Wiley, Hoboken, 2015), p. 712.
- [61] A. V. Khomenko and I. A. Lyashenko, *J. Phys. Stud.* **11**, 268 (2007).
- [62] A. V. Khomenko and O. V. Yushchenko, *Phys. Rev. E* **68**, 036110 (2003).
- [63] It is assumed that presence of oscillations around zero is due to the accuracy of calculations and the dimension of time series. It is considered that ACF decreases exponentially to a constant value, which equals to zero in the stationary case.